Experimental study of a novel solar multi-effect distillation unit using alternate storage tanks

M. Alsehli, B. Saleh, A. Elfasakhany, Ayman A. Aly and M. M. Bassuoni

ABSTRACT

In recent years, the use of solar energy has been growing exponentially and applied in a wider range of applications; one of the important applications for using solar energy is water desalination. The current work investigates the proof of concept experimental setup for a novel solar multi-effect distillation (MED) using alternate storage tanks. The experimental setup consists of a MED unit, two thermal storage tanks, and a solar collector. One storage tank is used as a charging tank while the other tank is used as a discharging tank. This unique dual-tank system stores the thermal energy to be used later in the MED unit, which improves the control of the water mass flow rate and water temperature throughout the MED process. The peak temperature achieved every day in the charging tank determines the MED production capacity. This system is designed for the tanks to alternate roles every 24 hours. The testing of this design was carried out during May 2019 in Saudi Arabia. The experimental results prove the novel concept design to work efficiently providing an average production rate of about 21 kg/day with total solar collector area of 2.7 m^2 and average daily performance ratio of 2.5.

Key words | multi-effect distillation, solar desalination, thermal storage, water production

M. Alsehli (corresponding author)
B. Saleh
A. Elfasakhany
Ayman A. Aly
Mechanical Engineering Department, College of Engineering,
Taif University,
P.O. Box 888, Taif,
Saudi Arabia
E-mail: *m.alsehli@tu.edu.sa*

B. Saleh
Ayman A. Aly
Mechanical Engineering Department, Faculty of Engineering,
Assiut University,
P.O. Box 71516, Assiut,
Egypt

M. M. Bassuoni
Mechanical Power Engineering Department, Faculty of Engineering,
Tanta University, El-Geish St. Tanta,
Egypt

NOMENCLATURE

ETC	Evacuated tube collector
CA	Collector area m^2
T_{si}	Medium fluid supply temperature, °C
T_{sr}	Medium fluid return temperature, °C
TBT	Top brine temperature, °C
T_{amp}	Ambient temperature, °C
PR	Performance ratio
RR	Recovery ratio, %
MED	Multi-effect distillation
M_d	Total distillate flow rate generated by the MED, kg/day
M_{sf}	Medium fluid mass, kg/day
M_f	Incoming mas of seawater, kg/day
I_s	Available solar power, Wh/m^2
V_w	Wind speed, m/s
h_{fg}	The water latent heat of vaporization in KJ/kg

doi: 10.2166/wrd.2020.068

INTRODUCTION

Background

The world's population is increasing rapidly, perhaps reaching about nine billion by the year 2050 (Ghiazza *et al.* 2013). This will increase the demand for fresh water by about twice (Bongaarts 2009). Thus, the demand for seawater desalination has become compulsory, especially in the areas where sources of fresh water are rare. Currently, the desalination process requires an intensive usage of fossil fuel, which emits bulky pollutants into our environment; additionally, new desalination units are being built every day with, of

course, increased use of fossil fuels. In the survey, approximately 19,000 desalination plants with 60 million cubic meters of capacity every day have been installed throughout the globe as of the year 2014 (Ghiazza *et al.* 2013). For a desalination plant to produce 13 million cubic meters of distillate water per day, it requires about 130 million tons of fuel per year (Eltawil *et al.* 2009; Gude 2015). In addition to the pollutants of fossil fuel, it costs a great deal to produce distillate water. In recent studies, it has been shown that to provide about 3% annual increment in the production of fresh water using desalination, an investment of about 500 billion dollars is needed (Shouman *et al.* 2015).

Generally, there are two techniques for water desalination processes. The first technique is phase-change, such as in the multi-stage flash (MSF) and/or multi-effect distillation (MED) systems, while the second technique is a single-phase, such as in the reverse osmosis (RO) systems. In the year 2010, for example, RO, MSF, and MED systems counted for 94% of worldwide desalination capacity (Calle *et al.* 2015). The MED process is commonly used in large thermal plants due to its low specific energy consumption and low top brine temperature (TBT), which usually ranges from 60 °C to 90 °C (Calle *et al.* 2015). Additionally, MED requires only half of the water pumping, compared with MSF, and that makes the MED process the most preferred one of the phase-change water desalination techniques (Frantz & Seifert 2015). The MED can be used for large-scale plants, similar to the plant which was installed in Jubail, Saudi Arabia in 2009, producing over 800,000 cubic meters per day (Clayton 2015).

MED operates by passing hot brine and steam through several sub-units; those sub-units are called 'effects'. Each sub-unit or effect contains a network of heat exchanger tubes, multiple nozzles (for spraying the brine over the heat exchanger tubes), and finally, a base pan to collect the brine.

Literature review

Currently, the world is moving towards replacing fossil fuel by renewable energy. However, renewable energy currently applied in water desalination is estimated to contribute only less than 1% of the desalination capacity worldwide (García-Rodríguez 2003). With the increasing costs of fossil fuel and its high pollutants, solar energy becomes more appropriate as a source for energy, especially new desalination units which are installed every day. In the literature, numerous studies have investigated the utilization of solar thermal energy in desalination units. Calle *et al.* (2015) investigated a dynamic model for a solar-assisted MED plant. A good agreement between simulation results and experimental data was obtained. Sharaf *et al.* (2011a) studied two different combined solar cycles with different configurations of MED processes. In the first technique, solar energy was utilized to power the MED process; in the second technique, the exhausted energy from the organic Rankine cycle turbine was used to power the MED process. The results showed that the second technique was more attractive than the first one. Joo & Kwak (2013) carried out a performance evaluation on a MED multi-effect distiller with 3 m^3/day capacity and shell-tube type heat exchanger. The results showed that the performance ratio of the developed distiller was about 2.02. Hu *et al.* (2019) carried out a comprehensive theoretical exergy analysis for the MED-reverse electrodialysis heat engine. The results showed that increasing the concentration of the initial brackish solution or the number of effects in the MED was helpful for improving the exergetic performance of the heat engine. Iaquaniello *et al.* (2014) developed an alternative scheme by proper integration of concentrating solar power with MED and RO desalination processes. The results showed that the desalination using concentrating solar power system through such hybrid integration allows for continuous operation and can be an effective way to lower water production costs. Andrés-Mañas *et al.* (2020) evaluated experimentally and performed a simulation analysis for a solar seawater desalination system. The simulated volume of distilled water generated annually ranged from 41.7 to 70.5 m^3. Hartwig & Sebitosi (2010) studied the feasibility and design of a solar-powered MED system. Furthermore, a simulation was constructed in order to predict the fresh water output. Sharaf *et al.* (2011b) evaluated solar power-assisted different techniques of MED-vapor compression processes. The results showed that reducing the value of the compression ratio with increasing the evaporator's numbers would reduce the specific power consumption, solar field area, and thermo-economic costs. Calise *et al.* (2014) investigated a solar system producing simultaneously electrical energy, thermal energy, cooling energy, and domestic water. The

results of the economic analysis were comparable with those reported for similar systems.

Li *et al.* (2013) reviews first solar desalination research activities, followed by discussions of solar-assisted desalination processes and a variety of possible combinations. They concluded that with the cost reduction of future solar systems and the development of novel solar technologies, as well as accurate solar radiation data collection and modeling, solar desalination could be an effective option for future desalination systems. Mohammadi *et al.* (2019) provided an overview of the status of state-of-the-art hybrid concentrated solar power desalination systems. The study demonstrated that there are many potential ways to hybridize concentrated solar power with desalination systems. Alhaj *et al.* (2017) carried out research and discussed the literature on a solar-powered MED, and highlighted key research drawbacks that should be considered. The design and simulation of a MED plant powered by a parabolic trough collector was presented by Mabrouk *et al.* (2013). The study concluded that the capital cost of groundwater was reduced by utilizing an air-cooled condenser.

A technical and economic study on MED-RO plant powered by solar energy that produces desalted water and electricity was conducted by Iaquaniello *et al.* (2014). The produced desalted water from the hybrid plant costs less than \$1.23/m^3. The performance of a linear Fresnel collector solar field integrated with a MED plant was modeled by Askari & Ameri (2016). A techno-economic analysis of the plant under different conditions was performed. Results revealed that the minimum water cost was obtained at the lowest solar share. An experimental study to characterize the performance of a MED thermal vapor compressor plant powered by a solar linear Fresnel collector was conducted by Hamed *et al.* (2016). It was found that to produce thermal energy of 13.6 MWh to the power plant, a solar field area of 55,737 m^2 was required. An optimized MED process driven by steam, which was provided by a linear Fresnel collector, was proposed by Alhaj *et al.* (2018). The results showed that the equivalent mechanical energy of the plant is 8 kWh/m^3, which is 59% lower than that of existing commercial MED facilities with thermal vapor compression. An innovative concept of a spray evaporation MED system, in which a spray evaporation tank was used to fully split brine disposal for water and salts was proposed by Guoa *et al.* (2020). Results indicated that a high evaporation efficiency of 99.86% was achievable by the modified spray evaporation tank. A novel concept of the integration of a MED for distillate generation with supercritical carbon dioxide Brayton cycle utilizing the waste heat from the power cycle was investigated by Sharan *et al.* (2019). For the different locations considered, Yanbu in Saudi Arabia gave the cheapest cost of the distillate and electricity generation. The distillate cost for the RO system is 16% higher compared with distillate produced by integrated MED. A low-temperature MED was proposed to improve the dispatch ability of a 600 MW coal-fired power generating unit by Xue *et al.* (2019). An unsteady thermal system model was developed to study peak shaving capacities. Braun & Kleffner (2019) studied MED to improve water management efficiency in several industry sectors. The study indicated that MED is a disruptive technology with regard to various industrial desalination challenges. Cui *et al.* (2019) applied an enumeration-based MED process synthesis framework for optimization utilizing column pressure as an independent decision variable. Results showed the MED can generally save nearly 50% of energy and up to 30% of the total annualized cost, compared to a conventional distillation column.

In comparison between the process of MED using fossil fuel and solar energy, in a solar desalination unit, the steam applied via the first effect is acquired through solar heat energy instead of through a boiler and/or an electric heater. The solar heat energy is transferred in the form of either thermal energy, as used in thermal storage technologies, or in the form of electrical energy, as used in photovoltaic (PV) technologies. The current work focuses on thermal solar desalination, e.g., using thermal storage technologies. In thermal solar desalination, there are generally two main approaches: direct solar desalination and indirect solar desalination. In direct solar desalination, solar energy is used to heat the brine directly, while in indirect solar desalination systems, solar energy is used to heat a medium fluid that passes through the brine within the heat exchanger. The current work uses the indirect thermal solar desalination process.

The use of solar energy requires application of a thermal storage system to manage daily variations in solar energy, and, in turn, the desalination plant could operate continuously throughout the day. Researchers proposed different thermal storage systems to drive the solar desalination

system. In our earlier study (Elfasakhany 2016), a nanocomposite energy storage system for increasing the performance and productivity of simple-type solar desalination was proposed. The results showed that the productivity was increased by about 125%. The current work investigates a novel thermal storage system design using two solar storage tanks with alternating roles. The first thermal tank is used as a charging tank while the second thermal tank is used as a discharging tank. The discharging tank is used for supplying hot medium fluid to the MED while the charging tank is used for holding the medium fluid that is circulated through the solar energy collectors and the two tank switch roles every day at sunset. This unique design aims to completely separate the MED from the solar energy variations over time and thus allows the MED unit to operate continuously and in the most efficient way. This novel concept was first numerically modeled and simulated by the authors in Alsehli *et al.* (2019), and the current experimental work serves as a continuation of the numerical modeling work and investigates the experimental proof of concept for this unique and novel design.

SYSTEM DESCRIPTIONS

The novel solar desalination system investigated in the current work consists of three subsystems: the first subsystem is the solar collector, the second subsystem is the thermal storage tanks, and the third subsystem is the MED unit. Figure 1 shows a schematic of the overall solar MED distillation unit. In this design, the brine is heated indirectly through a medium fluid that is stored in the alternate thermal storage tanks. In this section, the different subsystems and their roles in the desalination process are explained.

The first subsystem is the solar collector, which consists of an evacuated tube collector (ETC) that converts the solar energy into thermal energy that is absorbed by the medium fluid while circulating through the collector tubes. The circulating flow rate of the medium fluid is adjusted according to the heat that the collector can pass to the fluid to achieve the desired peak temperature. The heat value is a function of hourly ambient temperature, wind speed, *collector area*, and solar radiation intensity.

The second subsystem is the thermal storage system, which consists of two identical insulated tanks; each tank has enough capacity to feed the MED unit with the required amount of medium fluid for a full day. The first thermal tank is used as a charging tank while the second thermal tank is used as a discharging tank. During typical operation, the charging tank is designed to be full of hot medium fluid at sunset daily. This approach allows the charging tank to gradually raise the medium fluid temperature throughout the day, minimizing thermal losses to the environment. As the hot medium fluid from the discharging tank passes sensible heat to the MED unit, it undergoes a temperature change. This temperature change, along with the medium

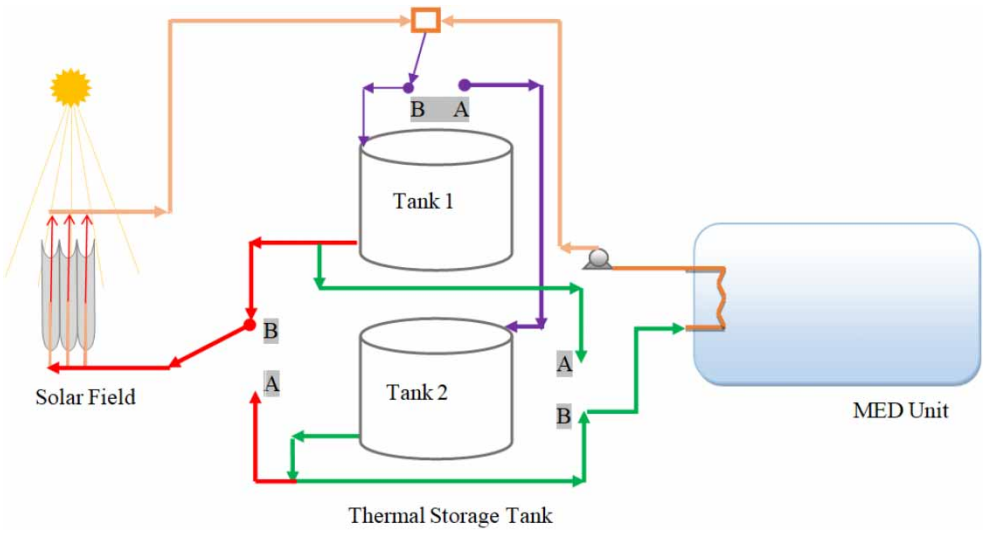

Figure 1 | Schematic of the overall solar MED distillation unit.

fluid flow, depends on the type of medium fluid, the effectiveness of the heat exchanger, the desired MED production level, and the top brine temperature in the first effect of the MED.

Figure 1 shows the operating principles of alternating thermal tanks. One tank is the charging tank, which is being filled with hot medium fluid that comes from the solar collectors; whereas the second tank is the discharging tank which feeds the MED with the hot medium fluid that was heated the day before (Joo & Kwak 2013). Every 24 hours, the tanks alternate roles as follows: if the two-way switch is in position 'A', this makes Tank 1 the discharging tank and Tank 2 is the charging tank; and if the two-way switch is in position 'B', this makes Tank 1 the charging tank and Tank 2 is the discharging tank.

The third subsystem is the MED, as shown in Figure 2. The heat exchanger in the first effect normally receives steam from an external heat source, such as a boiler for a power facility. This steam condenses within the heat exchanger in the first effect to heat and evaporate the feedwater. The steam and brine from the first effect are used to drive the second effect. Similarly, the steam from the second effect is used to drive the third effect, and so on, until the last effect. In this process, the distillate is being collected from the heat exchanger outlets via all effects in the system, except for the first one. The steam produced by the last effect is, consequently, passed through the condenser, which produces distillate and also pre-heats the incoming seawater for the system.

The MED in the current novel system accomplishes this duty with sensible heat from medium fluid stored in the discharging tank instead of the steam from an external heat source. The remaining MED operation is the same as a conventional MED, as explained above, e.g., vapor generated in the first effect is utilized as a heating source for the second effect, and vapor generated in the second effect is utilized as a heating source for the third effect, and so on to the last effect. The medium fluid is heated each day in the charging tank, by circulating through the solar collector, raising its temperature to a peak value that determines the MED production for the following day. Therefore, the MED should be able to accommodate daily changes in the medium fluid supply temperature.

EXPERIMENTAL SETUP

A schematic diagram for the solar MED unit with the alternate thermal storage tanks is shown in Figure 3, while Figure 4 shows a photograph of the experimental setup. The experimental setup was built and tested at Taif University, Taif, Saudi Arabia. As shown, the experimental setup consists of a MED unit, two thermal storage tanks, and an evacuated tube solar collector. The MED unit consists of three effects; each effect has a heat exchanger, a vapor

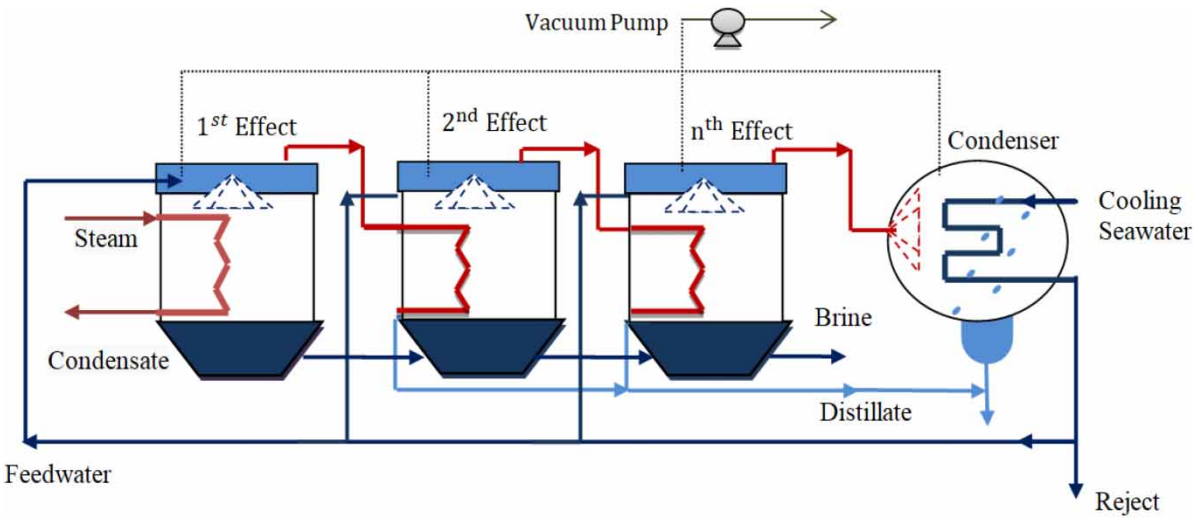

Figure 2 | A conventional MED layout.

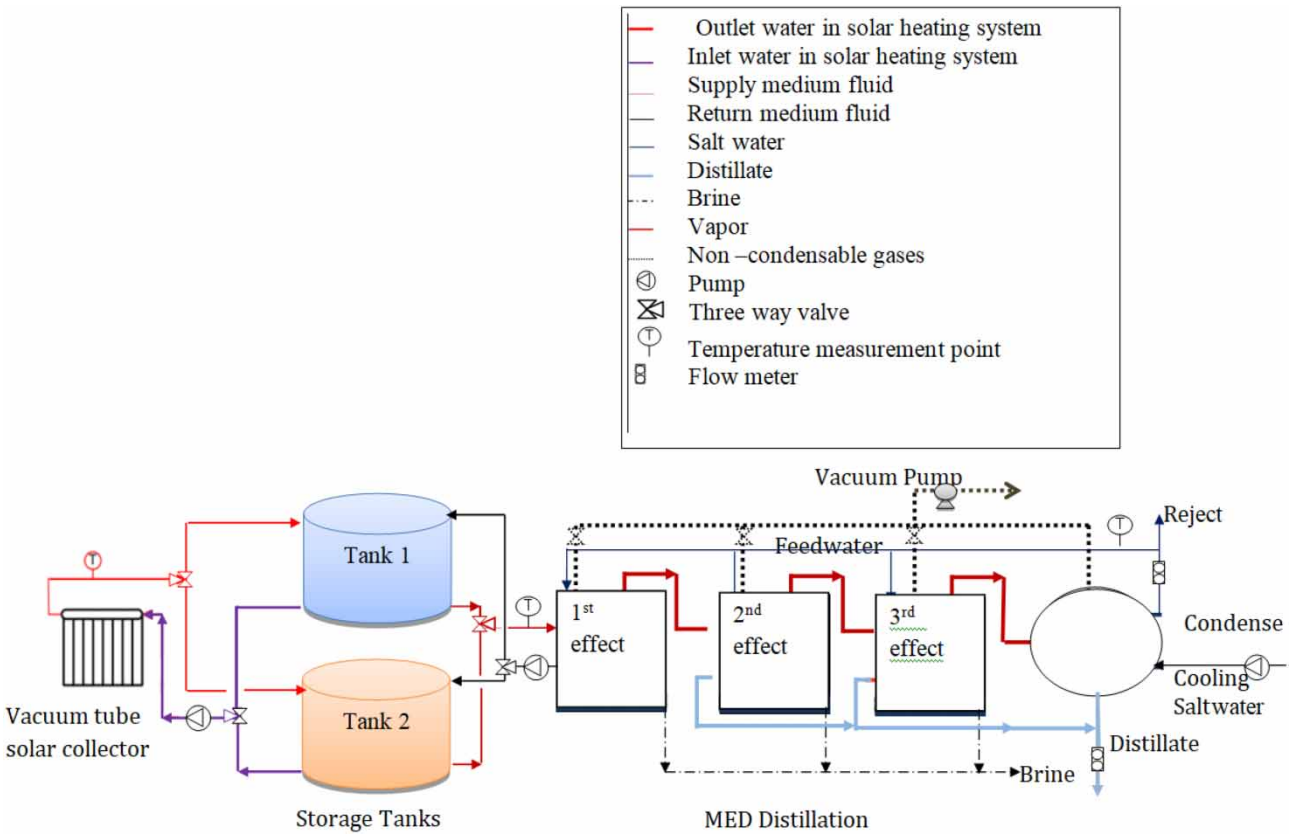

Figure 3 | Schematic diagram of the solar MED system.

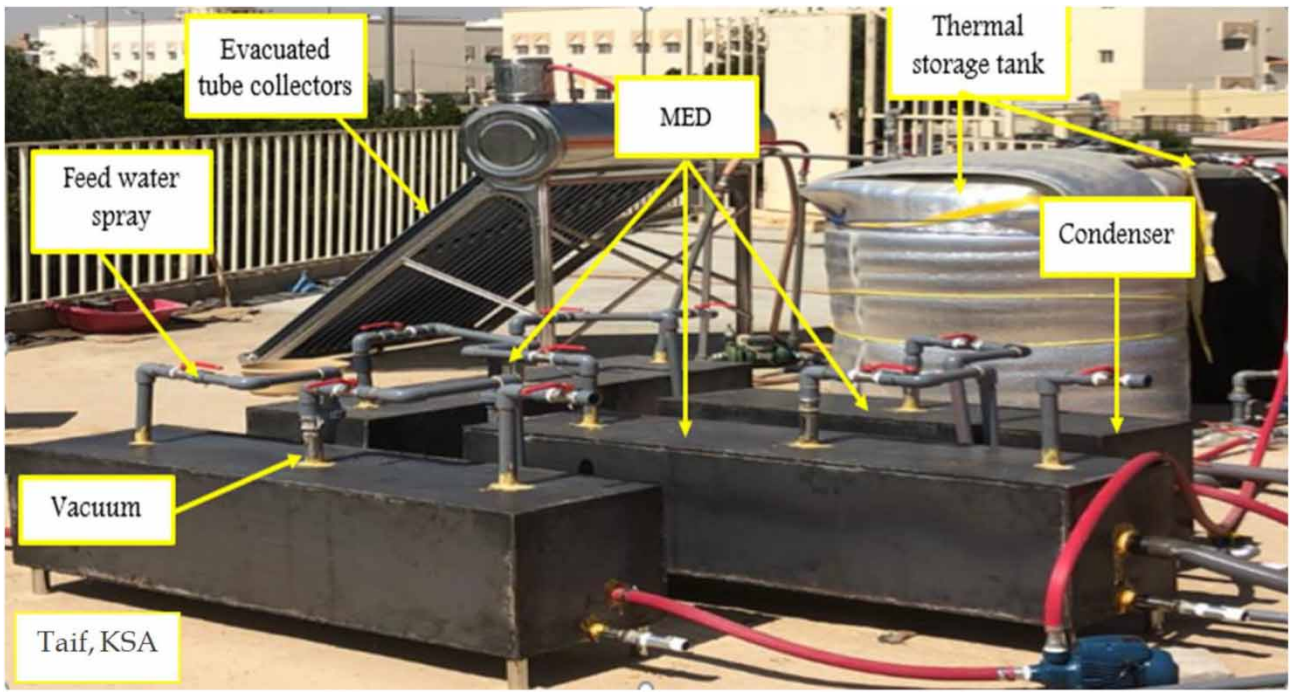

Figure 4 | A photograph of the experimental solar MED system.

space, a brine pool, a feedwater spray, and a condenser. The effect is a chamber made of galvanized iron and coated to prevent corrosion and reduces any thermal losses to the environment. The length, width, and height of each effect are 1.2 m, 0.4 m, and 0.4 m, respectively. The heat exchanger tubes across the effects are made from steel with a diameter of 0.5 inch. The incoming feedwater is partly preheated in the condenser by the vapor coming from the third effect which is fully condensed. The condenser consists of a chamber (1 m × 0.4 m × 0.4 m) made of galvanized iron sheet. The condenser tubes are designed similarly to the heat exchanger tubes and the outer surface of the condenser is completely insulated with proper insulating material. The desalinated water from the second effect, the third effect, and the condenser are collected by means of a flexible pipe into a measuring apparatus located next to the condenser.

The storage tanks used are cylindrical tanks made from sheet metal bending and soldering. The tanks are made of a galvanized iron sheet with 0.003 m thickness. The diameter and height of each tank are 1 m and 1.5 m, respectively, with a total volume of 1.18 m^3. To eliminate heat losses from the tanks the walls of the tanks are insulated by dense polyethylene material with a thickness of 0.015 m. The two thermal storage tanks are integrated with an evacuated tube solar collector with 2.7 m^2 surface area for heating the feedwater by absorbing the solar radiation. The technical specifications of the collector are given in Table 1. The solar collector is set up at a slope angle of 45° and facing in a south direction.

Table 1 | Technical specification of the evacuated tube collector

Part	Parameter	Value	Unit
Outer glass tube	Thickness	2	mm
	Diameter	47	mm
	Conductivity	0.74	W/m.k
	Length	1,500	mm
Inner glass tube	Thickness	2	mm
	Diameter	37	mm
	Conductivity	0.74	W/m.k
Copper tube	Thickness	0.7	mm
	Diameter	8	mm
	Conductivity	398	W/m.k
Absorbing coating	Absorptivity	0.92	–
	Emissivity	0.08	–

A vacuum pump is connected to the three effects and the condenser to create a vacuum pressure and remove any non-condensable gases at each effect and at the condenser. All the main components of the system are connected by 1-inch diameter PVC tubes while the distillate tank and the tank supplying the system with seawater are connected with a flexible pipe.

The experiment was carried out during the month of May in 2019 in Saudi Arabia. The testing was conducted over the course of the day starting around sunset at 7 p.m. when the thermal tanks switch roles. The tanks are designed to alternate roles at 7 p.m. so that the charging tank temperature gradually heats up to the peak temperature throughout the day.

The experiment was conducted with constant feedwater flow and constant medium fluid flow. Water flow meters were used to measure the flow rate of the medium fluid water, the feedwater, and the rejected brine while the distillate production was measured by the measuring apparatus. Temperature measurements throughout the system were taken using thermocouples, while the ambient temperature was measured by a laboratory mercury thermometer. The solar intensity was measured by a solar radiation solar meter and the wind speed was measured by a digital anemometer. The measuring instruments' characteristics are shown in Table 2. The distillate water, solar radiation, wind speed, temperature values, feedwater flow rate, medium fluid flow rate, and manometer measurements were all observed and recorded every hour.

RESULTS AND DISCUSSION

The experiment was conducted between May 23rd and May 31st in 2019, at Taif University, Taif, Saudi Arabia. Figure 5 shows the average daily variations of wind air speed over the duration of the experiment; as shown, the wind air speed tends to be more uniform over the course of the week and has an average value around 3.5 m/sec. Figure 6 shows the hourly variations of solar intensity measured between May 23rd and May 30th. As expected, the solar intensity starts increasing with the sun rise around 5 a.m. to 6 a.m. and reaches a peak value of 1,000 w/m^2 around 12 p.m., then decreases in the afternoon until all the solar intensity

Table 2 | Specification of the measuring instruments used in the experiments

Instrument	Type	Range	Measurement accuracy	Manufacturer
Water flow meter	12E	10–100 L/min	±1%	WAYSEAR
Solar power meter	TM – 207	2,000 W/m^2	±10 W/m^2	Tenmars
Air speed meter	GM8901	0–45 m/s	±3.0%	Benetech
Thermocouple	OM-EL	−200 to 390 °C	±1.0 °C	Omega

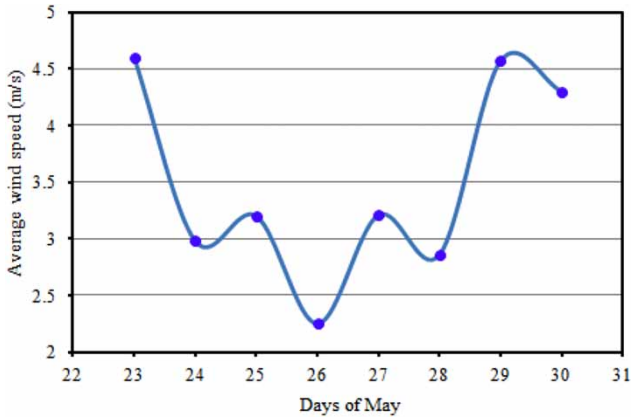

Figure 5 | Measured wind speed between 23rd and 30th May, 2019.

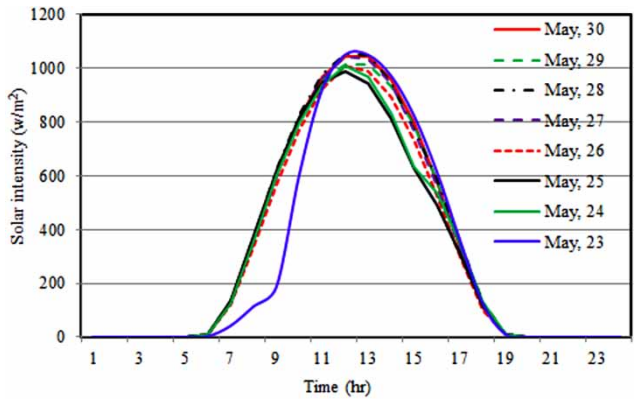

Figure 6 | Measured solar radiation between 23rd and 30th May, 2019.

fades away at sunset around 7 p.m. Between 8 a.m. and 5 p.m. every day, the solar intensity is in the range of 400–1,000 w/m^2.

A sample of the data collected and measured on May 26th is shown in Table 3. The average total solar irradiance obtained on the collector surface is about 8.23 kW.h/m^2 and the system produced a total of 21 kg/day of distillate water with the collector area of 2.7 m^2.

Table 3 | Data measured on May 26th

I_s (kW.h/m^2)	8.23
T_{amp} (°C)	33
V_w (w/s)	5.3
T_{sp} (°C)	71
M_f (kg/day)	50
A_c (m^2)	2.7
Md (kg/day)	21

Figure 7 shows the hourly cumulative production rate over the day of May 26th which adds up to about 19.5 kg with an average hourly production rate of about 0.8 kg/hr. As shown in the figure, the production rate rises linearly with time with a constant slope. This shows the continuous operation of the MED unit and the uniform production of distillate water independent from the variation in the solar energy throughout the day. This is only possible through the novel dual thermal tank alternating role design which completely separates the MED from the solar energy variations and allows the MED to operate continuously throughout the day providing a

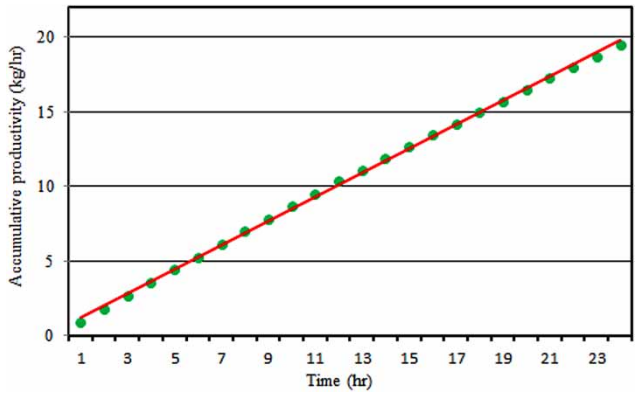

Figure 7 | Cumulative distillate production rate on May 26th 2019.

constant distillate product rate regardless of the solar energy variation.

To better correlate the variations in the distillate production with the solar intensity and the medium fluid supply temperature, Figure 8(a)–8(c), respectively, illustrate the collective bar graphs for the daily total solar intensity, medium fluid supply temperatures, and daily distillate production during the period of the experiment. It is seen that the average amount of solar irradiance varies between 285 W/m^2 and 325 W/m^2 with most of the average values around 305 W/m^2. It is also seen that the medium fluid supply temperature (the temperature of the discharging tank) follows the trend of solar irradiance with a 1-day shift, while the daily production rate follows the trend of the supply temperature on a day-to-day basis. It can also be seen that the highest supply temperature and hence the highest production rate occurred on May 29th, where it corresponds to the highest solar irradiance which occurred the previous day on May 28th. Similarly, it is shown that the lowest supply temperature and hence the lowest production rate occurred on May 24th where it corresponds to the lowest solar irradiance which occurred the previous day on May 23rd. This shows the medium fluid supply temperature and the daily distillate production rate are determined by the solar irradiance on the previous day.

To quantify the operation of the MED unit, a recovery ratio (*RR*) value is usually computed. The recovery ratio is defined as the ratio of distillate production rate to the incoming feedwater rate, which basically represents how efficient the distillation unit is in converting the feedwater into distillate water. The higher the recovery rate value, the better the operation effectiveness of the unit.

$$RR = \frac{Distillate\ Production\ (kg/s)}{Input\ Feedwater\ (kg/s)} \times 100 \tag{1}$$

Figure 9 shows the daily production rate (plotted on the primary right vertical axis) and the daily recovery rate values (plotted on the secondary left vertical axis) computed for the measured data. The results show that the daily *RR* has an average value of ~42% and that the maximum *RR* value of ~43% was computed on May 29th while the minimum *RR* value of ~40% was computed on May 24th. Those two dates correspond to the maximum and minimum measured solar intensity dates, respectively, during the period of conducting the experiment.

For further quantifying the operation of the MED unit, the performance ratio (*PR*) is usually computed as well. The *PR* is defined as the ratio of the power gained from the unit (distillate flow rate × latent heat of vaporization) with respect to the power input into the unit (El-Dessouky & Ettouney 2002; Joo & Kwak 2013):

$$PR = \frac{M_d \times h_{fg}}{Q} \tag{2}$$

where M_d is distillate flowrate, h_{fg} is the latent heat of the water evaporation, and Q (the power input) is the amount of heat required to raise the temperature of feedwater in the first effect. The 24-hourly average values of latent heat were calculated using experimental data:

$$Q(kW) = \dot{m}_{FS} \times C_p \times (T_i - T_o) \tag{3}$$

where $\dot{m}_{FS}$ is the mass flow rate of the medium supply fluid and T_i and T_o are the inlet and outlet temperatures of the medium fluid.

Figure 10 shows the daily values of *PR* for the measured data. The daily *PR* has an average value of 2.5 and the maximum *PR* value of 2.7 was computed on May 29th while the minimum *PR* value of 2.3 was computed on May 24th. Those dates correspond to the maximum and minimum measured solar intensity dates, respectively, during the period of conducting the experiment.

In order to evaluate the performance of a solar integrated multi-effect distillation, the specific energy consumption should be adopted. The specific thermal energy consumption (*SEC*) for the MED plant can be expressed as:

$$SEC = \frac{Q\,(kW)}{M_d\,(kg/s)} \tag{4}$$

where M_d is distillate flowrate h_{fg} is the latent heat of the water evaporation, and Q is the useful heat gain by the working fluid. The 24-hourly average values of latent heat were calculated using experimental data. Figure 11 illustrates

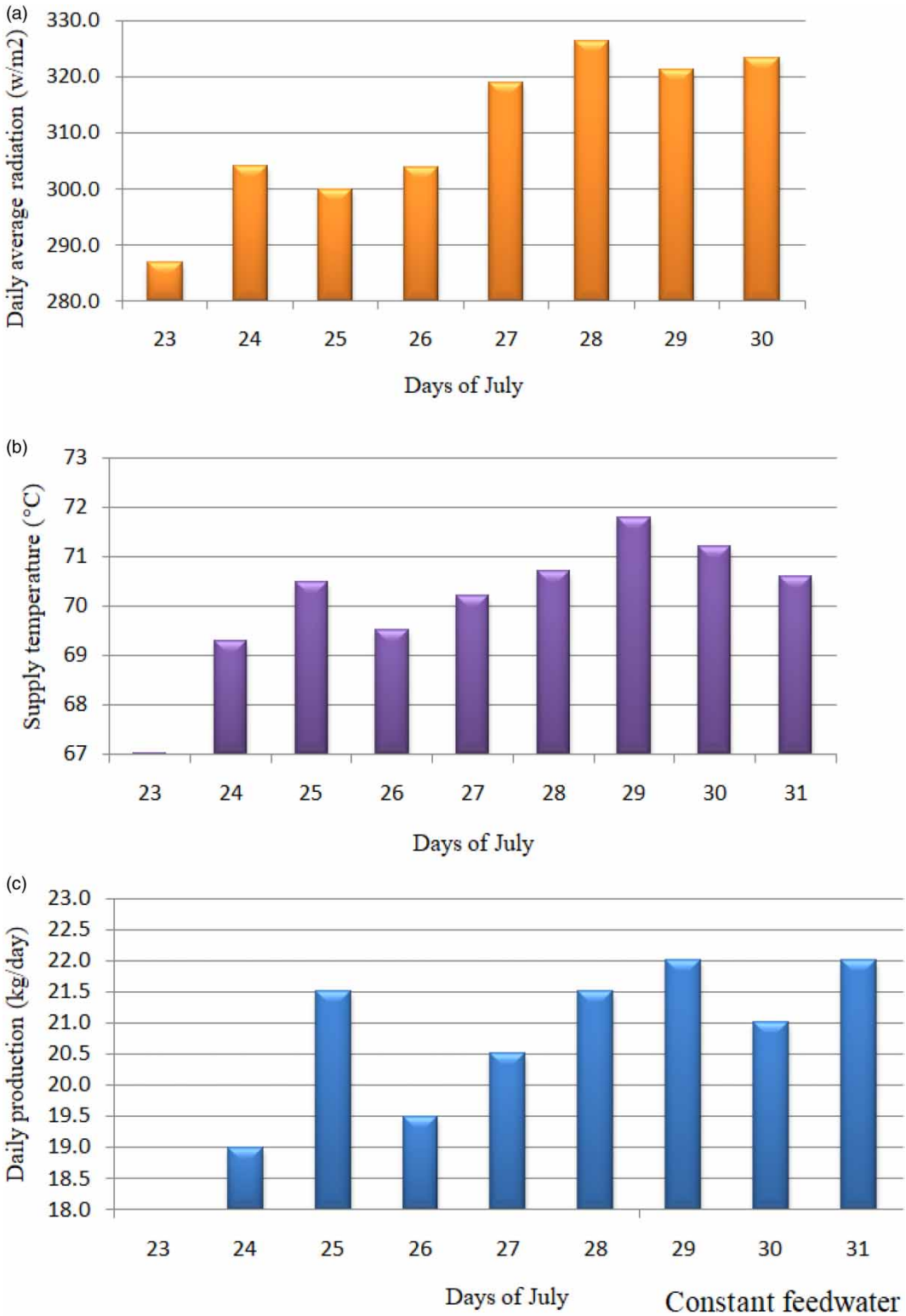

Figure 8 | (a) Measured solar radiation and solar irradiance between May 23rd and May 30th, (b) medium fluid supply temperature between May 24th and May 31st, and (c) daily distillate production between May 24th and May 31st.

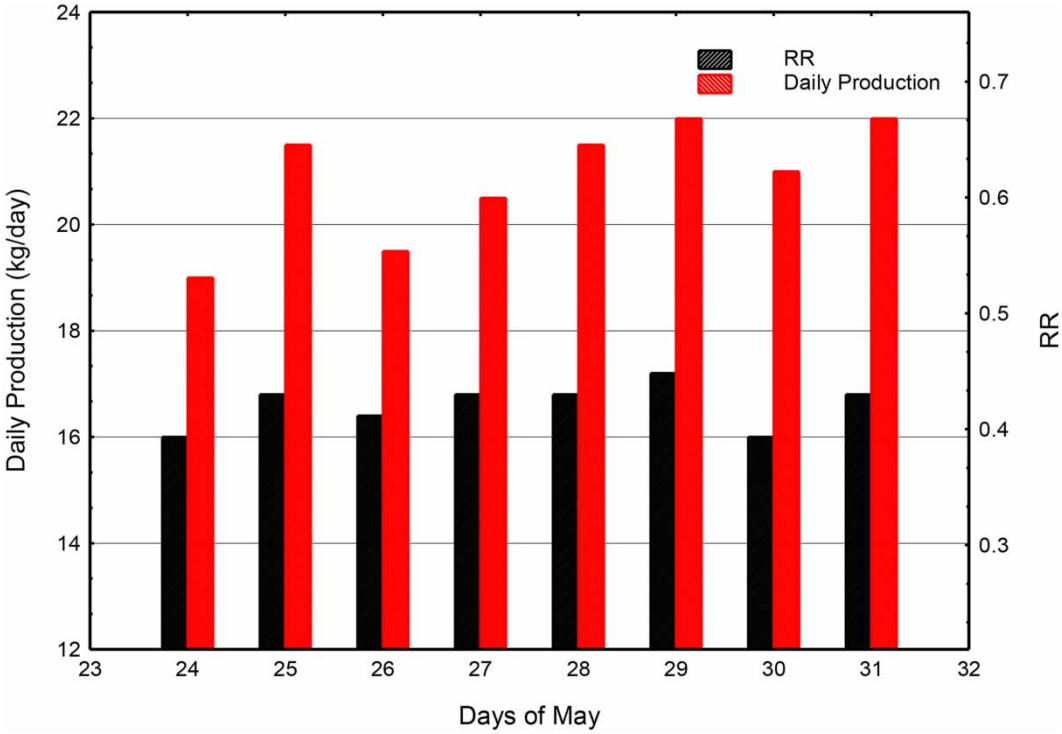

Figure 9 | Variations of total distillate production rate and recovery ratio (*RR*).

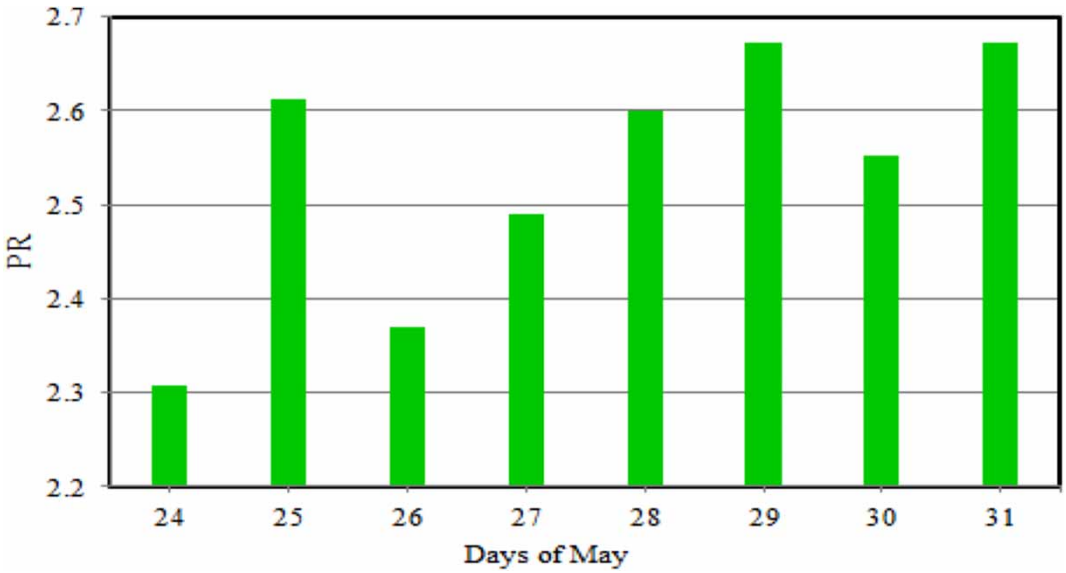

Figure 10 | Computed performance ratio for the solar MED system between May 24th and May 31st.

the computed daily values of *SEC* for the measured data. It is seen that the daily *SEC* has an average value of 831 kJ/kg and that the maximum *SEC* value of 911 kJ/kg was computed on May 24th while the minimum *SEC* value of 786 kJ/kg was computed on May 29th. Those dates correspond to the minimum and maximum measured solar

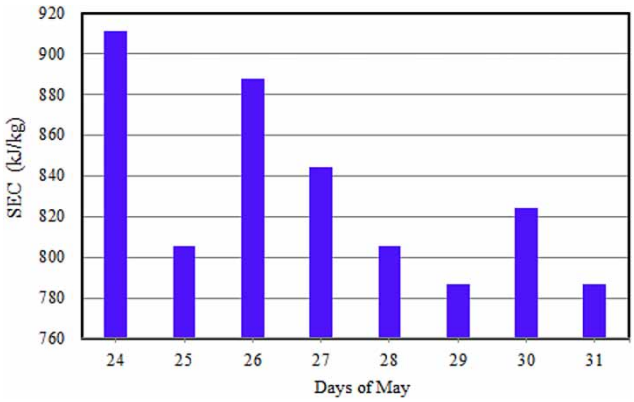

Figure 11 | Computed SEC for the solar MED system between May 24th and May 31st.

intensity dates, respectively, during the period of conducting the experiment.

To compare the current solar MED performance with other experiments (Leblanc *et al.* 2010), the published data of a recent experiment with the same number of effects and the same supply temperature (noting the difference in the solar collector area and thus the production rate) was selected for an A-to-B comparison as shown in Table 4. The current solar MED has a better recovery rate and lower specific thermal energy values.

CONCLUSIONS

A novel solar-powered multi-effect desalination system was built, tested, monitored, and evaluated. The system includes two tanks where one tank is used for solar charging while the other tank is used for feeding the MED. The two thermal tanks switch roles at the end of the day. The discharging tank is designed to contain an adequate amount of the medium fluid at a temperature suitable for running the process for a full day. In the meantime, the charging tank receives the medium fluid back from the first effect and circulates it through the solar collector to increase its temperature gradually. The experiment was conducted from May 23rd to May 31st in 2019 in the western region of Saudi Arabia. The distillate water, solar radiation, wind speed, temperature values, feedwater flow rate, medium fluid flow rate, and manometer measurements were all observed and recorded every hour. The recovery ratio, the performance ratio, and specific energy consumption were computed for the system throughout the testing duration period.

The results from the experiment show the system works effectively with good efficiency of this parallel-arrangement MED system. The system produces an average of 21 kg/day of distillate with an average daily performance ratio of 2.5 and an average specific thermal energy consumption of 831 kJ/kg. The novel dual-tank alternating role design completely separates the MED from the solar energy variations and allows the MED to operate continuously throughout the day, providing a constant distillate product rate regardless of the solar energy variation. For future work, it is recommended to look into the necessary steps to industrialize this novel solar-powered multi-effect desalination system.

Table 4 | Comparison of performance of two experiments

Parameter (unit)	Experiment (Leblanc *et al.* 2010)	Current experiment
Number of effects	3	3
Freshwater yield (kg/day)	1,460	21
Area of solar pond/collector (m^2)	720	2.7
Supply temperature (°C)	70	71
Specific thermal energy consumption (kJ/kg)	912	831
Recovery rate (%)	41	42
Performance ratio	–	2.5

ACKNOWLEDGEMENTS

The authors appreciate the support from Taif University (Grant No. 1-439-6073). The authors would also like to thank the Department of Mechanical Engineering at Taif University for providing the experimental facilities used in the current work.

REFERENCES

Alhaj, M., Hassan, A., Darwish, M. & Al-Ghamdi, S. G. 2017 A techno-economic review of solar-driven multi-effect distillation. *Desalination and Water Treatment* **90**, 86–98.

Alhaj, M., Mabrouk, A. & Al-Ghamdi, S. G. 2018 Energy efficient multi-effect distillation powered by a solar linear Fresnel collector. *Energy Conversion and Management* **171**, 576–586.

Alsehli, M., Mussad, A. & Jun-Ki, C. 2019 A novel design for solar integrated multi-effect distillation driven by sensible heat and alternate storage tanks. *Desalination* **468**, 114061.

Andrés-Mañas, J. A., Roca, L., Ruiz-Aguirre, A., Acién, F. G., Gil, J. D. & Zaragoza, G. 2020 Application of solar energy to seawater desalination in a pilot system based on vacuum multi-effect membrane distillation. *Applied Energy* **258**, 114068.

Askari, I. B. & Ameri, M. 2016 Techno economic feasibility analysis of Linear Fresnel solar field as thermal source of the MED/TVC desalination system. *Desalination* **394**, 1–17.

Bongaarts, J. 2009 Human population growth and the demographic transition. *Philosophical Transactions of the Royal Society B: Biological Sciences* **364** (1532), 2985–2990.

Braun, G. & Kleffner, C. 2019 Industrial water desalination by vacuum multi-effect membrane distillation. *Chemie Ingenieur Technik* **91** (10), 1400–1408.

Calise, F., Dentice d'Accadia, M. D. & Piacentino, A. 2014 A novel solar trigeneration system integrating PVT (photovoltaic/thermal collectors) and SW (seawater) desalination: dynamic simulation and economic assessment. *Energy* **67**, 129–148.

Calle, A., Bonilla, J., Roca, L. & Palenzuela, P. 2015 Dynamic modeling and simulation of a solar-assisted multi-effect distillation plant. *Desalination* **357**, 65–76.

Clayton, R. 2015 *Desalination for Water Supply FR/R0013. A Review of Current Knowledge*. Foundation for Water Research, Marlow, UK, pp. 1–50.

Cui, C., Xi, Z., Liu, S. & Sun, J. 2019 An enumeration-based synthesis framework for multi-effect distillation processes. *Chemical Engineering Research & Design: Transactions of the Institution of Chemical Engineers Part A* **144**, 216–227.

El-Dessouky, H. T. & Ettouney, H. M. 2002 *Fundamentals of Salt Water Desalination*, 1st edn. Elsevier Science BV, Amsterdam, The Netherlands.

Elfasakhany, A. 2016 Performance assessment and productivity of a simple-type solar still integrated with nanocomposite energy storage system. *Applied Energy* **183**, 399–407.

Eltawil, M. A., Zhengming, Z. & Yuan, L. 2009 A review of renewable energy technologies integrated with desalination systems. *Renewable and Sustainable Energy Reviews* **13** (9), 2245–2262.

Frantz, C. & Seifert, B. 2015 Thermal analysis of a multi effect distillation plant powered by a solar tower plant. *Energy Procedia* **69**, 1928–1937.

García-Rodríguez, L. 2003 Renewable energy applications in desalination: state of the art. *Solar Energy* **75** (5), 381–393.

Ghiazza, E., Borsani, R. & Alt, F. 2013 Innovation in multistage flash evaporator design for reduced energy consumption and low installation cost. In: *International Desalination Association World Congress on Desalination and Water Reuse*, Tianjin, China.

Gude, V. G. 2015 Energy storage for desalination processes powered by renewable energy and waste heat sources. *Applied Energy* **137**, 877–898.

Guoa, P., Lia, T., Lib, P., Zhaia, Y. & Lia, J. 2020 Study on a novel spray-evaporation multi-effect distillation desalination system. *Desalination* **473**, 114195.

Hamed, O. A., Kosaka, H., Bamardouf, K. H., Al-Shail, K. & Al-Ghamdi, A. S. 2016 Concentrating solar power for seawater thermal desalination. *Desalination* **396**, 70–78.

Hartwig, G. R. & Sebitosi, A. B. 2010 *Design of A Solar Powered Desalination System for use in South Africa*. Stellenbosch University, Stellenbosch, South Africa.

Hu, J., Xu, S., Wu, X., Wu, D., Jin, D., Wang, P., Xu, L. & Leng, Q. 2019 Exergy analysis for the multi-effect distillation – reverse electrodialysis heat engine. *Desalination* **467**, 158–169.

Iaquaniello, G., Salladini, A., Mari, A., Mabrouk, A. A. & Fath, H. E. S. 2014 Concentrating solar power (CSP) system integrated with MED–RO hybrid desalination. *Desalination* **336**, 121–128.

Joo, H. J. & Kwak, H. Y. 2013 Performance evaluation of multi-effect distiller for optimized solar thermal desalination. *Applied Thermal Engineering* **61** (2), 491–499.

Leblanc, J., Andrews, J. & Akbarzadeh, A. 2010 Low-temperature solar-thermal multi-effect evaporation desalination systems. *International Journal of Energy Research* **34** (5), 393–403.

Li, C., Goswami, Y. & Stefanakos, E. 2013 Solar assisted sea water desalination: a review. *Renewable and Sustainable Energy Reviews* **19**, 136–163.

Mabrouk, A., Fath, H., Iaquaniello, G. & Salladini, A. 2013 Simulation and design of MED desalination plant with air cooled condenser driven by concentrated solar power. In: *International Desalination Association World Congress on Desalination and Water Reuse*, Tianjin, China.

Mohammadi, K., Saghafifar, M., Ellingwood, K. & Powell, K. 2019 Hybrid concentrated solar power (CSP)-desalination systems: a review. *Desalination* **468**, 114083.

Sharaf, M. A., Nafey, A. S. & García-Rodríguez, L. 2011a Exergy and thermo-economic analyses of a combined solar organic cycle with multi effect distillation (MED) desalination process. *Desalination* **272** (1–3), 135–147.

Sharaf, M. A., Nafey, A. S. & García-Rodríguez, L. 2011b Thermo-economic analysis of solar thermal power cycles assisted MED-VC (multi effect distillation-vapor compression) desalination processes. *Energy* **36** (5), 2753–2764.

Sharan, P., Neises, T., McTigue, J. D. & Turchi, C. 2019 Cogeneration using multi-effect distillation and a solar-powered supercritical carbon dioxide Brayton cycle. *Desalination* **459**, 20–33.

Shouman, E. R., Sorour, M. H. & Abulnour, A. G. 2015 Economics of renewable energy for water desalination in developing countries. *Journal of Engineering Science and Technology Review* **5** (1), 1–5.

Xue, Y., Ge, Z., Yang, L. & Du, X. 2019 Peak shaving performance of coal-fired power generating unit integrated with multi-effect distillation seawater desalination. *Applied Energy* **250**, 175–184.

First received 25 November 2019; accepted in revised form 1 February 2020. Available online 17 March 2020